Proceedings of the ASME 2008 International Design Engineering Technical Conferences & Computers and Information in Engineering Conference
IDETC/CIE 2008
August 3-6, 2008, Brooklyn, New York, USA

DETC2008-49559

THE DEVELOPMENT OF AN INCREMENTALLY LOADED FINITE ELEMENT MODEL OF THE WHOLE SKIN LOCOMOTION MECHANISM: DISCOVERING THE RELATIONSHIP BETWEEN ITS SHAPE AND MOTION

Derek Lahr
RoMeLa: Robotics & Mechanisms Laboratory
Mechanical Engineering Department
Virginia Polytechnic and State University
Blacksburg, Virginia 24061
Email: dlahr@vt.edu

Dennis Hong[1]
RoMeLa: Robotics & Mechanisms Laboratory
Mechanical Engineering Department
Virginia Polytechnic and State University
Blacksburg, Virginia 24061
Email: dhong@vt.edu

ABSTRACT

The Whole Skin Locomotion (WSL) robotic platform is a novel biologically inspired robot that uses a fundamentally different locomotion strategy than other robots. Its motion is similar to the cytoplasmic streaming action seen in single celled organisms such as the amoeba. The robot is composed of a closed volume, fluid filled skin which generally takes the shape of an elongated torus. When in motion the outer skin is used as the traction surface. It is actuated by embedded smart material rings which undergo cyclical contractions and relaxations, generating an everting motion in the torroidially shaped skin. To better understand, design, and optimize this mechanism, it is necessary to have a model of the skin, fluid, and actuators and their interactions with the environment. This paper details the first steps in the development of a non-linear finite element (FE) model which will allow us to study these interactions and predict the shape and motion of the robot under various actuation strategies. A simple membrane element model is introduced from literature and is modified such that an incremental loading strategy can be employed. Finally, an underlying physical mechanism is introduced which could possibly describe the relationship between the shape of and pressure within the membrane skin and motion of the whole skin locomotion robot.

1 INTRODUCTION

1.1 Background

The Whole Skin Locomotion (WSL) robotic platform [1] is a novel biologically inspired robot that uses a locomotion strategy analogous to the cytoplasmic streaming motion seen in single celled organism. The body of the WSL mechanism consists of a toroid shaped skin filled with liquid. The fluid filled toroid model is like that of a common child's toy that is often referred to as a "water worm." When the robot is in motion, the outer skin is used as the traction surface, propelling the robot in relation to its environment. Upon reaching the aft end of the robot, the skin everts, and travels through the center of the robot to the stern. At this point the skin exits the center of the robot and returns to the outside where the cycle begins again.

This transportation mechanism is inspired by the way some single celled amoeboid organisms move, such as the *Amoeba proteus* (giant amoeba) or *Chaos chaos*. The motion of these organisms is generated by a process of liquid to solid and solid to liquid transformation of the organisms body itself which is called cytoplasmic streaming. In this process, the liquid endoplasm flows inside the ectoplasmic tube and transforms into the gel-like ectoplasm outer skin at the front. The ectoplasm outer skin at the end transforms back into the liquid form endoplasm at the rear. The net effect of this continuous ectoplasm-endoplasm transformation is the forward motion of the amoeba [2].

The technology to implement a similar transformation on any scale does not yet exist. Instead, the WSL uses the everting motion described earlier, in which the outer skin turns itself

1. Address all correspondence to this author.

inside out and returns to the front of the robot through the robot center. Therefore the robot is necessarily torroidially shaped and can be thought of as a three dimensional tank tread. By turning itself inside out in a single continuous motion, the overall motion of the cytoplasmic streaming ectoplasmic tube in amoebae can be replicated as illustrated in Figure 1.

1.2 Motion Generation Mechanism

The motion of the torus shaped skin is generated by the contraction and expansion of actuation rings embedded in the skin. There are currently two methods being considered for this application. On a large scale, larger than .1[m], accordion like pneumatic rings embedded in the skin which expand and contract with changes in pressure can be utilized [2]. This method can deliver both the high strains and forces that would be necessary to generate motion in the WSL robot. On a small scale, rings of electroactive polymers (EAP) would be placed around the circumference of the toroid to drive the motion. Because EAPs cannot generate both large displacements and forces, these materials are limited to small scale implementations. At this point, the focus of the research is on the smaller scale designs, and from here on only the EAP actuators will be considered.

As was stated earlier, this robot is fluid filled, and therefore its shape and motion are determined by the fluid pressure, the tension in the skin, and the force generated by the actuators embedded in the skin. For example, from rudimentary experiments with the "water worm" toy, we would expect that a generally contractile force generated by these EAP strips at the rear of the robot to cause this end to taper down and generate a forwards motion.

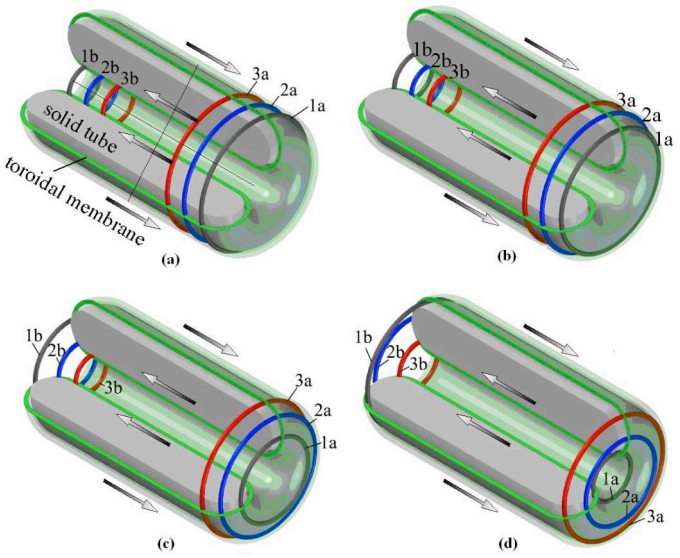

Figure 1. Everting motion of the WSL robot. Note that the solid tube pictured has been replaced with fluid in current design iterations. [2]

At this point though, we have no way to quantify this motion or the shape generated by the internal forces. Stated differently, the interactions between the skin, fluid, ground, and actuators are not well understood. Therefore we are not able to predict the shape or motion of this robot when the EAP strips are actuated. It is then of course difficult to control, let alone design the robot. This is the driving force behind the research to develop a finite element model which can incorporate the statics and dynamics of the hyper-elastic skin, fluid filled interior, and the smart material actuators. It is also hoped that the development of the FEA model will give us some insight into the underlying mechanisms within the skin and fluid that generate this motion.

The goal of this research project is to have a model to which we can apply actuator forces and predict the resulting shape and motion of the robot. This paper details several objectives of the research, which were as follows: 1) gain an understanding of finite element models used for membrane surfaces; 2) implement a suitable model in Matlab® with an appropriate loading strategy; 3) find the final shape of the robot and predict its motion; 4) introduce an analytical solution and compare it to the FEA results to gain insight into the fundamental mechanisms that propel this robot.

Developing our own FEA code will allow us to have more control to enforce volume constraints, implement buckling models, and develop our own elements. We also hope to gain a fundamental understanding of the mechanics of the WSL robot that would otherwise not be possible. Thirdly, we can corroborate our results with commercial software, further validating the model.

2 MEMBRANE BASED FINITE ELEMENTS

Finite element methods are numerical procedures to obtain solutions to complex engineering problems [3]. They are particularly useful when modeling complex phenomenon and/or complex geometries where analytical models are cumbersome and difficult. As mentioned earlier, of particular interest to us is the interaction of the membrane with the actuators, fluid interior, and ground. Therefore at this point, only the membrane is modeled, and the other bodies which dynamically interact with the membrane are modeled as prescribed forces or displacements within the FE model.

The membrane described here is a flat, thin structure which exhibits only in-plane stresses and no bending stiffness [4,5]. Therefore any out of plane stresses applied to the membrane, such as the internal fluid pressure, are counteracted by a geometric stiffness rather than a material stiffness. That is, out of plane forces are transformed to in-plane stresses through the geometry of the membrane. Membranes also have no compressive stiffness, therefore the membrane is quite susceptible to wrinkling and buckling, a feature which should be noted is not yet included in this analysis. It is believed that the buckling and wrinkling mechanisms are crucial to the motion of the WSL robot and will be incorporated in the future.

One possible method to accomplish this is presented by Ziegler [6].

2.1 Element formulation

The element model presented within this paper was originally presented by Arcaro [7]. In this formulation, the mesh consists of triangular elements, each with three nodes having three degrees of freedom apiece. From the displacements, the strain is derived using Green's strain which results in a non-linear formulation of elements. At this point in time, a linear Hookean elastic material model is used to develop the strain energy equation; however, a non-linear material model will be implemented in the future to better represent the actual mechanics of the WSL robot membrane.

Arcaro's model also uses triangular shaped elements within which the state of strain does not vary. A single element and its nodal displacements appear as in Figure 2.

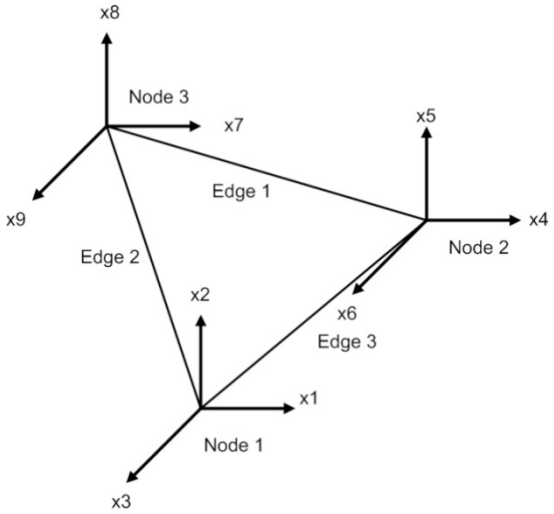

Figure 2. Triangular element used for 3-D analysis.

Arcaro's work is clever in that instead of representing the strains within the element as two normal strains and a shear strain, he uses three normal strains in the direction of the edges of the triangle. In this way the plane in which the element lies is not significant. Said differently, there exists a transformation [C] such that Equation 1 is true:

$$\begin{Bmatrix} e_1 \\ e_2 \\ e_3 \end{Bmatrix} = \begin{bmatrix} C^2(\theta_1) & S^2(\theta_1) & \sqrt{2}C(\theta_1)S(\theta_1) \\ C^2(\theta_2) & S^2(\theta_2) & \sqrt{2}C(\theta_2)S(\theta_2) \\ C^2(\theta_3) & S^2(\theta_3) & \sqrt{2}C(\theta_3)S(\theta_3) \end{bmatrix} \begin{Bmatrix} e_{xx} \\ e_{yy} \\ e_{xy} \end{Bmatrix} = [C] \begin{Bmatrix} e_{xx} \\ e_{yy} \\ e_{xy} \end{Bmatrix} \quad (1)$$

where e_1, e_2, and e_3 are the strains along the element edges 1, 2, and 3 as seen above in Figure 8, e_{xx} and e_{yy}, are the strains in the *x* and *y* direction respectively, e_{xy} is the shear strain in the *xy* plane, and θ_1, θ_2, and θ_3 are the angles of edges 1, 2, and 3 with respect to the x-axis. Using Arcaro's derivation, the actual orientation of the element within the *xy* plane is not important and instead, the internal angles of the triangular element are used.

The strain energy for each element, *e*, can then be computed as in Equation 2:

$$\varphi_e = \int_{Volume} \frac{1}{2} \begin{Bmatrix} e_1 \\ e_2 \\ e_3 \end{Bmatrix} [C]^{-T}[H][C]^{-1} \begin{Bmatrix} e_1 \\ e_2 \\ e_3 \end{Bmatrix} dV \quad (2)$$

where [H] is a matrix of material properties relating the stress to strain and dV is the differential volume element. Because the strains are constant across the element, the integral can be evaluated easily. In this clever way, the plane in which the element lies is built into the matrix [C] and the strain energy within each element can be computed. Therefore it follows that [C] must be computed for each element and is the only component of the formulation that takes into account the position of each node. All further calculations only use the displacements of each node. Each of the strain values, e_1, e_2, and e_3, are given by Equation 3 which is essentially the definition of Green's strain [8]:

$$e_i = \frac{2\{u\}^t\{z_i\} + \{z_i\}^t\{z_i\}}{2} \quad (3)$$

where $\{u_i\}$ is the unit vector along side *i* of the element where *i*=1:3, and $\{z_i\}$ is given as in Equations 4-6.

$$\{z_1\} = \frac{(\{x_3\} + \{px_3\}) - (\{x_2\} + \{px_2\})}{\lambda 1} \quad (4)$$

$$\{z_2\} = \frac{(\{x_1\} + \{px_1\}) - (\{x_3\} + \{px_3\})}{\lambda 2} \quad (5)$$

$$\{z_3\} = \frac{(\{x_2\} + \{px_2\}) - (\{x_1\} + \{px_1\})}{\lambda 3} \quad (6)$$

where $\{x_i\}$ is the vector containing the three Cartesian displacements of the *i*th node of element, which appears across from the *i*th edge as in Figure 2. The vector $\{px_i\}$ is a vector containing the sum of all previous displacements for that node. To be clear, the resulting vector, $\{e_1, e_2, e_3\}$ is defined for each element, and is a function of nine displacements, three displacements for each of the three nodes that make up the element. It is at this point that our formulation differs from Acaro's. Because we must use an incremental loading strategy, it is necessary to store at least one vector for each node which contains the magnitude and direction of the sum of all previous displacements. In this way, when the total potential energy is summed throughout the structure, it will take into account the path taken by the nodes and the total strain within each element [9].

As with most finite element formulations, the solution is the minimum point of the potential energy function, where the total energy for the entire model is given as in Equation 7:

$$\pi = \sum_1^m \varphi_e - \{f\}^t\{x\} - \{pf\}^t\{px\} \qquad (7)$$

where {x} is the vector containing the three Cartesian displacements of all the nodes in the model and therefore has length 3n where n is the number of nodes, *m* is the number of elements, and *{f}* is the vector of nodal forces applied at this particular loading iteration. Finally, the product, $\{pf\}^t\{px\}$, is the work done by all previous externally applied loads. It is therefore represented as the sum of the products of the applied nodal forces, *{pf}*, and associated displacements, *{px}*. This term is of little importance though because it is a constant for the current iteration, and will vanish when Equation 7 is differentiated. As stated earlier though, it is important not to neglect the strain energy built up in the membrane from previous iterations.

2.2 Using the Newton-Rhapson Method

Looking at Equation 4, one can see that there is a non-linear term, $\{z_i\}^t\{z_i\}$. This makes the formulation of a conventional stiffness matrix very difficult. Instead, a Newton-Rhapson method was used to solve the system of equations given by Equation 8, which states that the gradient of Equation 7 must be zero:

$$\frac{\delta\pi}{\delta x_i} = 0 \qquad (8)$$

where x_i is one of the nodal displacements [10]. The solution to Equation 9 will yield the local minimum of the potential energy equation and therefore the stable point of the structure. In order to solve this system it is necessary to generate the Jacobian of Equation 9 which for clarity has the form given by Equation 9 [11]:

$$J(\pi) = \begin{bmatrix} \frac{\delta^2\pi}{\delta x_1 \delta x_1} & \cdots & \frac{\delta^2\pi}{\delta x_1 \delta x_{3n}} \\ \vdots & \ddots & \vdots \\ \frac{\delta^2\pi}{\delta x_{3n} \delta x_1} & \cdots & \frac{\delta^2\pi}{\delta x_{3n} \delta x_{3n}} \end{bmatrix}. \qquad (9)$$

Representing the Jacobian mathematically is straightforward, but the actual computation of such a matrix is quite complex considering each element of the Jacobian can be a function of up to *3n* variables. A complete detailed description of this work is outside the scope of this paper. To summarize here though, an element-wise pattern was established which related the indices of each element in the Jacobian matrix to one of nine possible solutions for the second derivative of the strain vector, $\{e_1, e_2, e_3\}$ for each element. In this way, the code can assemble a local Jacobian matrix for each element and add it to the total system Jacobian matrix. A similar pattern was also established for the first derivative of the strain vector as seen in the gradient vector as well.

Newton's method is an iterative method. A guess must first be formulated, the gradient and Jacobian calculated, and then an update to that guess can be solved from the linear system given by Equation 10:

$$J(\pi, \{x\}^p)(\{x\}^{p+1} - \{x\}^p) = \left\{\frac{\delta\pi(\{x\}^p)}{\delta x_i}\right\} \qquad (10)$$

where $\{x\}^p$ is the best guess to the displacements of the p^{th} iteration of the Newton-Rhapson method. As the Jacobian should be symmetric, Matlab's PCG routine can be used to solve each step [12]. This routine is particularly useful because the size of the Jacobian is 3n x 3n and therefore for large membranes, the size of the Jacobian can become very large. Using the updated solution vector, $\{x\}^{p+1}$, the Jacobian and gradient are recomputed and the program solves for another more accurate update vector. A solution is found when the update vector, $(\{x\}^{p+1}-\{x\}^p)$, is sufficiently small that the iterative procedure can be terminated. The displacement vectors can then be added to the nodal positions and then displayed or processed further.

3 LOADING CONDITIONS

As alluded to earlier, the loading of a highly elastic structure must be done carefully, especially when the direction of the loads is closely related to the shape of the structure, as with the normal force generated from an internal pressure. Being that this model contains both an internal pressure and a highly elastic membrane structure, great care was taken to ensure the loads were appropriately applied.

3.1 Incremental Loading

The method used herein is generally called "incremental loading." As the name implies, the load is gradually and incrementally increased from zero to its final value. At each iteration, the direction and magnitude of the load are updated for the most recent configuration and nodal location. In this way, as the membrane is "inflated" from its static, unstressed position, the direction of the pressure loads acting on the surface can be updated.

The two dominant loading mechanisms in this model were the pressure loading, and the circumferential stress contributed by the EAP actuators. The loads from the actuators were applied radially to nodes placed at the location of the actuators themselves. It is therefore fairly straightforward to compute the nodal forces from these loads.

The pressure loads were handled differently. Both the direction and magnitude of the nodal forces resulting from the pressure were based off the area vector of each element. The formulation is given simply as in Equation 11,

$$\begin{Bmatrix} f_{ix} \\ f_{iy} \\ f_{iz} \end{Bmatrix} = \begin{Bmatrix} f_{ix} \\ f_{iy} \\ f_{iz} \end{Bmatrix} + \frac{P}{3} \begin{Bmatrix} A_{ix} \\ A_{iy} \\ A_{iz} \end{Bmatrix} \quad (11)$$

where f_{ix}, f_{iy}, f_{iz} are the components of the force vector applied to the ith node in the x, y and z direction respectively. Similarly, $\{A_{ix}, A_{iy}, A_{iz}\}$ is the area vector normal to the surface of the element and P is the magnitude of the internal pressure. The force vector appears recursively in this definition, because as the program cycles through the elements computing the forces, it is easiest to sum the forces on one node of an element with the previously computed forces on that node from the adjacent elements. Once the pressure loads have been determined, the loads from the actuators are added to the pressure loads at the respective nodes.

At this point the only interactions with the ground considered were that with the portion of the membrane on the internal side of the robot. That is to say that the interior of the WSL robot can be thought of as being fixed to a pipe. This simplification was made so that the intricacies of the model would not be overwhelming. It is believed though that the fundamental physics underlying the everting motion can still be ascertained from this simplified model. In reality, the reaction force will most likely be generated by the friction from the weight of the robot on a flat surface. The fundamental physics of the everting motion though should remain the same regardless of the application site of the reaction force. Figure 3 shows the unloaded cylindrical membrane structure. The cylinder ends are fixed in all three directions in this case. This is nearly equivalent to affixing the inner surfaces of the elongated torus to the aforementioned pipe on which the WSL robot is moving.

3.2 Incremental Iteration Termination

It is of course necessary to determine a point of termination of the incremental loading strategy. We chose to end the algorithm when the volume within the membrane reached a certain value. This is derived from the fact that the WSL robot is filled with a fluid that is assumed to be incompressible. Therefore any configuration that the membrane takes must have the same total volume. Using each element as one side of four of a tetrahedron, and assuming an arbitrary fixed point in the interior of the WSL model as the final vertex of that tetrahedron, the volume of said robot can be found as in Equation 12,

$$V = \frac{1}{3!}\sum_{i=1}^{n} \begin{vmatrix} xp_{i1} & yp_{i1} & zp_{i1} & 1 \\ xp_{i2} & yp_{i2} & zp_{i2} & 1 \\ xp_{i3} & yp_{i3} & zp_{i3} & 1 \\ xp_f & yp_f & zp_f & 1 \end{vmatrix} \quad (12)$$

where xp_{ij} , yp_{ij}, zp_{ij} with $i,j=1:3$ are the Cartesian coordinates of the j^{th} nodes of element i and x_f , y_f, z_f, are the coordinates of a fixed point in the center of the robot. Using this formulation, it is only necessary that the specified fixed point forms a line of sight with every node of the model and that no line crosses through any of the other elements.

Therefore, after each step of the incremental loading, the volume is calculated. The final few steps are then a refinement of the loads to hone in on the correct volume to the desired accuracy.

4 PRELIMINARY FEA RESULTS

The program was first run for six incremental steps, each one with an increasing pressure. No actuator loads were considered initially to reduce the chance of error. The mesh size was refined over several runs until convergence was achieved. For these preliminary models, a mesh with eleven rings, each with ten nodes proved satisfactory. The mesh size was reduced at the ends of the model in order to achieve better resolution and more accurately model the curvature at the ends of the robot. Figures 3 through 5 show the progression of the inflation from an unstressed state to a fully inflated form.

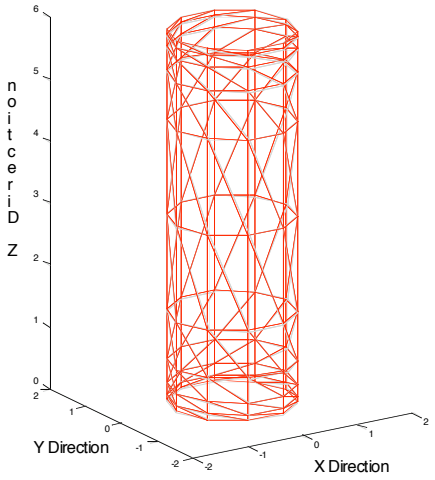

Figure 3. Initial configuration of the unstressed WSL membrane.

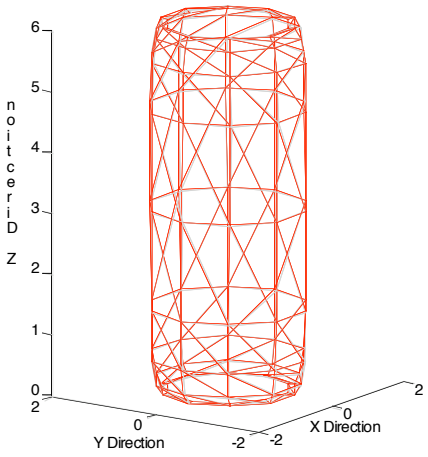

Figure 4. Partially inflated membrane.

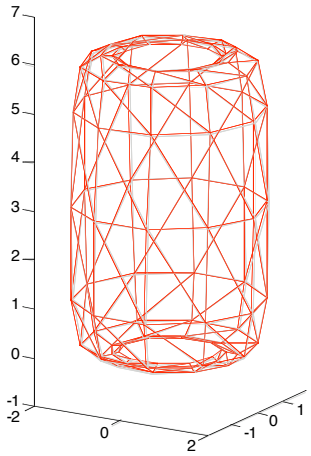

Figure 5. Fully inflated membrane.

The ballooning action of the membrane is as we would have expected. We see that from Figure 3 to Figure 4, the cylinder begins to stretch in the radial direction, but at this point the ends have not rolled over, and the defining torroidial shape of the WSL robot has not been reached. With increased internal pressure, as seen in Figure 5, the membrane becomes fully inflated while the ends have formed the "caps" of the elongated torus shape. We believe that the caps of the elongated torus are fundamental to the everting motion of this robot because they form the transition from the inner membrane (the fixed interior of this model) to the outer membrane. Therefore, any forces generated which allow the inner membrane to move in relation to the outer membrane or vice versa should pass through this membrane. It is therefore important that they appear in the model as the membrane is inflated. One mechanism we believe can describe these interactions is described in the following section.

After the initial inflated but unactuated membrane shape had been verified, the actuator loads were applied. These loads were applied to nodes on only one end of the robot in an inwardly radial direction. As discussed in the introduction, this loading mimics the contractile force generated by EAP actuators. Loading only one end of the membrane ensures we see an asymmetric shape that can generate a forwards motion. To maintain the volume constraint, the internal pressure was also increased from the previously described loading strategy. Figure 6 shows the actuated results as compared to the unactuated shape in Figure 5.

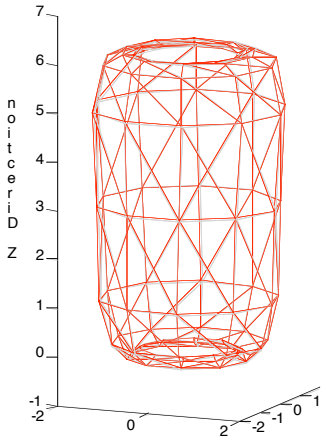

Figure 6. Membrane under applied pressure and actuator loads exhibiting the characteristic tapered shape as compared to Figure 5.

Studying Figure 6, one can see a slightly tapered shape of the lower section of the robot that results from the actuator loads on that end. The numerical results are more interesting. To predict the motion of the robot, we looked at the maximum and minimum position of the membrane with respect to the fixed nodes, which are located at 0 and 6[in] on the z-axis. When unactuated, the membrane was symmetric about the midplane of the robot, with the curved torus caps extending 0.086[in] beyond these ends. When loaded though, the lower end extended as far as 0.2[in] below the lower fixed nodes, and the upper end receded such that it was only .07[in] above the upper fixed nodes. In other words, we can observe that the outer membrane moved down in the negative *z* direction as much as .1[in] with respect to the inner membrane. Therefore if the outer membrane were fixed, by the static friction between itself and the ground for instance, we would see the inner membrane advancing forward, causing a net forward motion of the robot. These results confirm the accuracy of the membrane model with respect to rudimentary physical experiments [1] with the water worm in that they both show similar fundamental relationships between their shape and motion.

5 ANALYTICAL PRESSURE VESSEL MODEL

In developing this finite element model we hope to have a benchmark or method of comparison as the underlying physical model is researched. The primary mechanism being studied, which could explain the motion of the WSL robot, will be briefly introduced here. It is a pressure vessel model of the membrane which compares the hoop stresses of the forward and rearward torus ends.

The WSL robot is fundamentally a pressure vessel in which the pressure is developed within the fluid through the elastic deformation of the membrane. It follows then that a pressure vessel model of the motion could be developed. Rather than looking at the motion though, the forces generating this motion are considered. Figure 7 shows a sagittal cross section of the WSL robot. A small section of the inner and outer membranes are fixed through which the reaction forces are developed. The fixed condition of the outer membrane represents the robots interaction with the ground, while the reaction force generating the motion is quantified through the fixed condition of the inner membrane.

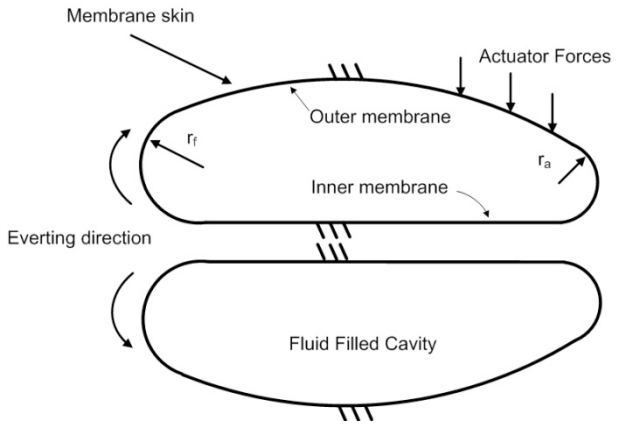

Figure 7. Sagittal section of WSL robot with actuator loads applied and portions of the inner and outer skin fixed.

A free body diagram, as seen in Figure 8, of the inner membrane will help us relate the reaction force responsible for the motion and the stresses in the inner membrane. The pressure load and its reaction normal to the membrane have no effect on this portion of the skin and thus is omitted for clarity.

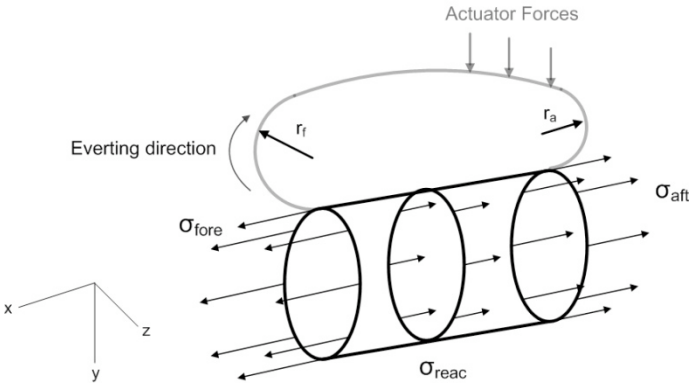

Figure 8. Free body diagram of the robots inner membrane.

Knowing that the hoop stress is proportional to the radius for a given thickness and pressure [13] and that the radius of the forward section is greater then that of the aft section, $r_a<r_f$, due to the constricting effect of the actuators on the aft membrane, we can say that $\sigma_{fore}>\sigma_{aft}$. Therefore the reaction stress, σ_{reac}, will be in the negative direction. In the absence of this fixed condition and the resulting stress, the inner membrane will move in the positive x direction causing a net forward motion of the robot in relation to the ground.

Although this theory explains the origin of the driving force, at this point it unfortunately helps us little in terms of finding the magnitude of that force and its relationship to the actuator forces. Further study is needed to analytically relate the actuator forces to the shape of the membrane, such that this driving force relationship can be completed. It is in this study that the FEA model will be extensively used.

6 CONCLUSIONS

The Whole Skin Locomotion robotic platform is a novel biologically inspired robot that uses a fundamentally different locomotion strategy than other robots. Its strategy is similar to the cytoplasmic streaming motion seen in single celled organism such as the amoeba. This novel locomotion strategy requires unique modeling procedures to understand the interactions between the robot skin, fluid filled interior, the actuators within the skin, and the surrounding environment. With a more complete model of the robot, it can be designed and optimized for its novel form of locomotion.

This paper detailed the development of a non-linear finite element (FE) model which will allow us to study the interaction of the membrane and actuators and predict the shape and motion of the robot under various actuation strategies. A simple membrane element was developed and an incremental loading strategy employed to model the displacement dependent pressure and actuator loads. The loading iterations were terminated once the membrane reached a certain volume. At each step, a Newton-Rhapson solver was used to determine the shape of the membrane. It was shown that a strictly contractile

force at the aft end of the robot will generate a forwards motion. An underlying physical mechanism based on the hoop stress within the membrane was introduced which could possibly describe the relationship between the shape of the membrane skin and motion of the whole skin locomotion robot.

ACKNOWLEDGMENT

The authors would like to thank the National Science Foundation for their support for part of this work under Grant No. 0643839.

REFERENCES

[1] Ingram, M. and Hong, D. W., "Whole Skin Locomotion Inspired by Amoeboid Motility Mechanisms", 29th ASME Mechanisms and Robotics Conference, Long Beach, California, September 24-28, 2005.
[2] Ingram, M. and Hong, D. W., "Mechanics of the Whole Skin Locomotion Mechanism Concentric Solid Tube Model: the Effects of Geometry and Friction on the Efficiency and Force Transmission Characteristics", 30th ASME Mechanisms and Robotics Conference, Philadelphia, Pennsylvania, September 10-13, 2006.
[3] Segerlind, J., "Applied Finite Element Analysis," John Wiley and Sons, New York, 1984.
[4] Spillers, W.R., Schologel, M., Pilla, D., "A Simple Membrane Finite Element," Computers and Structures, Vol. 45, No. 1, 1992.
[5] Schweizerhog, K., Ekkehard, R., "Displacement Dependent Pressure Loads in Nonlinear Finite Element Analysis," Computers and Stuctures, Vol. 18, No. 6, 1984.
[6] Zieger, R., Wagner, W., Bletzinger, K., "A Finite Element Model for the Analysis of Wrinkled Membrane Structures," International Journal of Space Structures, Vol. 18, No. 1, 2003.
[7] Arcaro, V.F., "A Simple Procedure for Shape Finding and Analysis of Fabric Structures." http://www.arcaro.org/tension/index.htm., 2007.
[8] Batra, R. C., "Elements of Continuum Mechanics," American Institute of Aeronautics and Astronautics, Reston Va, 2006.
[9] Zienkiewicz, O.C., Taylor, R.L., "Finite Element Method for Solid and Structural Mechanics," Butterworth-Heinemann, Burlington, MA, 2005.
[10] Kelley, C.T.,"Solving Nonlinear Equations with Newton's Method", Society for Industrial and Applied Mathematics, Philadelphia PA, 2003.
[11] Marsden, J.E., Tromba, "Vector Calculus," W. H. Freeman and Company, New York, 2003.
[12] van der Vorst, H. A., "Iterative Methods for Large Linear Systems," Cambridge University Press, New York, 2003.
[13] Beer, F.P., Johnston, E.R., DeWolf, J.T., "Mechanics of Materials," McGraw-Hill, New York, NY, 2001.